Clim Dyn (2013) 41:2411–2426
DOI 10.1007/s00382-012-1616-5

Validating a regional climate model's downscaling ability for East Asian summer monsoonal interannual variability

Tomonori Sato · Yongkang Xue

Received: 17 July 2012 / Accepted: 26 November 2012 / Published online: 7 December 2012

Abstract Performance of a regional climate model (RCM), WRF, for downscaling East Asian summer season climate is investigated based on 11-summer integrations associated with different climate conditions with reanalysis data as the lateral boundary conditions. It is found that while the RCM is essentially unable to improve large-scale circulation patterns in the upper troposphere for most years, it is able to simulate better lower-level meridional moisture transport in the East Asian summer monsoon. For precipitation downscaling, the RCM produces more realistic magnitude of the interannual variation in most areas of East Asia than that in the reanalysis. Furthermore, the RCM significantly improves the spatial pattern of summer rainfall over dry inland areas and mountainous areas, such as Mongolia and the Tibetan Plateau. Meanwhile, it reduces the wet bias over southeast China. Over Mongolia, however, the performance of precipitation downscaling strongly depends on the year: the WRF is skillful for normal and wet years, but not for dry years, which suggests that land surface processes play an important role in downscaling ability. Over the dry area of North China, the WRF shows the worst performance. Additional sensitivity experiments testing land effects in downscaling suggest the initial soil moisture condition and representation of land surface processes with different schemes are sources of uncertainty for precipitation downscaling. Correction of initial soil moisture using the climatology dataset from GSWP-2 is a useful approach to robustly reducing wet bias in inland areas as well as to improve spatial distribution of precipitation. Despite the improvement on RCM downscaling, regional analyses reveal that accurate simulation of precipitation over East China, where the precipitation pattern is strongly influenced by the activity of the Meiyu/Baiu rainfall band, is difficult. Since the location of the rainfall band is closely associated with both lower-level meridional moisture transport and upper-level circulation structures, it is necessary to have realistic upper-air circulation patterns in the RCM as well as lower-level moisture transport in order to improve the circulation-associated convective rainfall band in East Asia.

Keywords Regional climate modeling · Dynamical downscaling · East Asian summer monsoon · Atmosphere–land interaction

T. Sato (✉)
Faculty of Environmental Earth Science, Hokkaido University, Kita-10, Nishi-5, Sapporo 060-0810, Japan
e-mail: t_sato@ees.hokudai.ac.jp

Y. Xue
Department of Geography, University of California, Los Angeles, CA, USA

Y. Xue
Department of Atmospheric and Oceanic Sciences, University of California, Los Angeles, CA, USA

1 Introduction

Motivated by societal and scientific demands for climate information with higher resolution, research using regional climate models (RCMs) has developed rapidly since early limited-area atmospheric models were applied to climate research (Dickinson et al. 1989; Giorgi and Bates 1989). Recently, dynamical downscaling using regional atmospheric models has expanded its range of application from short-term weather prediction, seasonal to interannual variability, and global warming (e.g., Giorgi et al. 2001) to paleo-climate (e.g., Diffenbaugh et al. 2006). RCMs are

now widely applied as promising tools for downscaling coarse-resolution gridded data supplied from reanalysis data or general circulation model (GCM) experiments.

Castro et al. (2005) classified dynamical downscaling experiments with respect to constraints imposed on RCMs, namely initial conditions and boundary conditions, and contemplated the advantage of using RCMs, i.e., whether dynamical downscaling adds value to the imposed lateral boundary conditions (LBC). For the Type 1 experiment, in which initial conditions have a principal effect on the simulated result, it is evident that the regional model has achieved significant progress in numerical weather prediction. However, for dynamical downscaling with constraints of greater degrees of freedom (types 2, 3, and 4 experiments classified in Castro et al. 2005), in which the effect of initial conditions is no longer dominant and LBCs from a reanalysis or GCM's seasonal to longer climate simulations provide constraints on the RCM large scale circulation, further investigations are required on how the RCM retains or adds value. Castro et al. (2005) and many other papers discussed adding value problem of the dynamically downscaled data for a rather small spatial and time scale. Because this is the core issue in any dynamical downscaling, we have extend the investigation of this issue to much longer time scale and larger spatial scale (Xue et al. 2007). In this paper, our main theme is only for the seasonal time scale and continental spatial scale but we still keep the same definitions for different downscaling categories as proposed by Castro et al. (2005).

There are several factors which affect uncertainty of the result in the dynamical downscaling. In order to quantify possible causes of deficiency in downscaling generated by RCM-derived errors, it is useful to adopt reanalysis data as boundary forcing, which is referred to as a perfect boundary experiment (or type 2 experiment in Castro et al. 2005). There are many studies evaluating the value added by dynamical downscaling with the perfect boundary experiment (e.g., Castro et al. 2005; Fu et al. 2005; Xue et al. 2007; Gao et al. 2011). In addition to errors due to the quality of lateral boundary condition data (e.g., Gong and Wang 2000; Xue et al. 2012), known sources of uncertainty generated through RCM experiments are horizontal resolution (e.g., Christensen et al. 1998; Mo et al. 2000; Wang et al. 2003; Zhang et al. 2003; Castro et al. 2005; Xue et al. 2007; Sato et al. 2008), domain size and location (e.g., Treadon and Petersen 1993; Xue et al. 2007; Gao et al. 2011), lateral boundary settings (Denis et al. 2003; Giorgi and Mearns 1999; Warner et al. 1997), and physics schemes (Xue et al. 2001; Liang et al. 2004; Wang et al. 2004). Meanwhile, the nudging setup (including nudging method and coefficient for time scale) has been introduced to overcome the problems caused by the above mentioned factors (e.g., Marbaix et al. 2003; Gong and Wang 2000; Xu and Yang 2012). The RCM's ability to add value in East Asian regional climate downscaling, where the region covers complex topographical features, has been extensively investigated. For instance, Gao et al. (2011) tested the RCM's dynamical downscaling ability in an extreme flood event during the summer of 1998 using a set of numerical experiments with different land surface and cumulus schemes, initialization methods, and locations of the lateral boundary. Kang and Hong (2008) investigated the sensitivity of simulated climatology to convective parameterizations. Fu et al. (2005) conducted the RCM inter-comparison project (RMIP), in which nine RCMs participated, and found that cumulus parameterization is the most important factor that causes diversity of simulated regional climate in East Asia. Ishizaki et al. (2012) examined the RCM's ability to simulate the Japanese climate using five RCMs. They found the RCMs tend to overestimate weak rainy days and underestimate heavy rainy days. Those studies focused on the RCM's performance in downscaling intra-seasonal to seasonal variations, usually dealing with a typical weather event or climatological mean state. However, with substantial interannual variability in the Earth's climate system, the results of dynamical downscaling revealed in the previous studies are likely dependent on the climate conditions during the target year/period. For example, the role of land surface processes on precipitation strongly depends on the land surface conditions in the targeting year/period (Kanae et al. 2001; Sato and Kimura 2007). Therefore, the downscaling investigations targeting a select year/period are insufficient to lead to a general conclusion about the RCM's performance. It is important to evaluate the RCM's performance for multiple years and to clarify the influence of interannual variability on the RCM's downscaling ability. We speculate that the RCM should have different performance for dry years and wet years. This hypothesis will be tested in this study.

In this study, the RCM's ability to dynamically downscale seasonal means is evaluated first. Then our evaluation extends to multiple years in order to take into account the influence of year-to-year variation of environmental factors on performance of dynamical downscaling. The analysis and experimental domain covers East Asia (Fig. 1) which consists of five sub-domains,[1] Mongolia (90–120°E, 42–52°N), Southeast China (S.E. China; 105–120°E, 22–28°N), North China (N China; 105–120°E, 32–38°N), Northwest China (N.W. China; 90–105°E, 35–41°N), and the Tibetan Plateau (90–105°E, 28–34°N). The five sub-domains contain a variety of climate categories: cold and

[1] We define the sub-domain names here for convenience in the presentation. Some sub-regions cover several countries and/or regions.

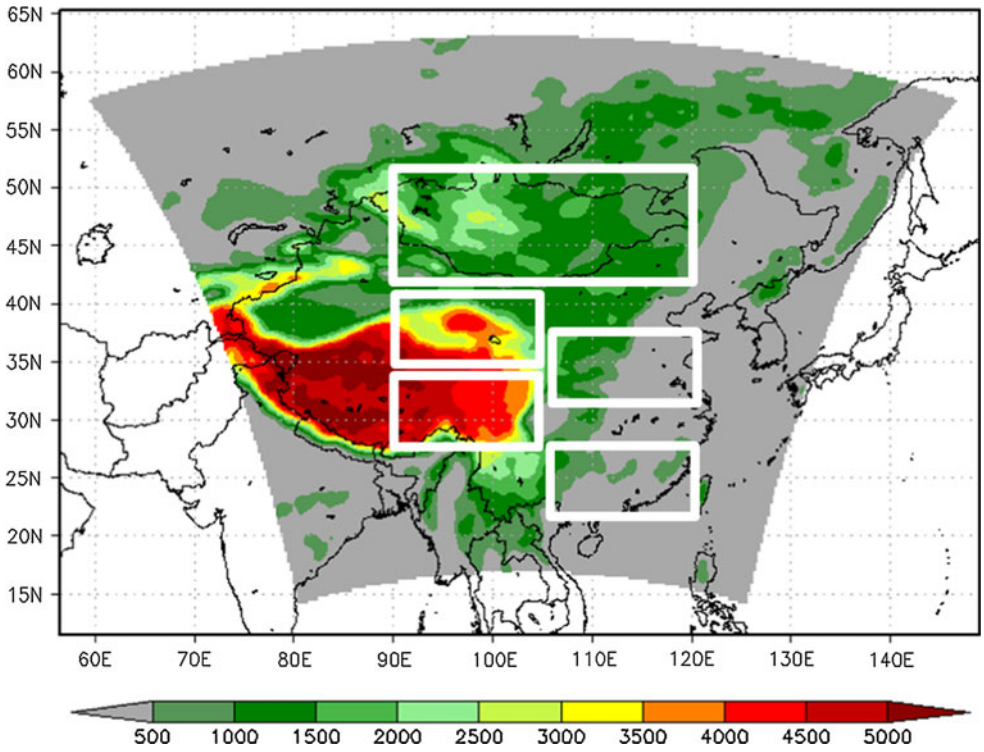

Fig. 1 Topography in study area and experimental domain. *Rectangles* show sub-domains for analysis; Mongolia (90–120°E, 42–52°N), Southeast China (105–120°E, 22–28°N), North China (105–120°E, 32–38°N), Northwest China (90–105°E, 35–41°N), and Tibetan Plateau (90–105°E, 28–34°N)

dry area, mountain area, tropical humid plain area, and the transition zone. The RCM's downscaling ability in each subregion will be evaluated and compared. This study mainly focuses on the investigation of the RCM's performance in simulating the East Asian summer monsoon (EASM) during June–July–August (JJA). A measure of statistical indices representing atmospheric circulation and precipitation is introduced for quantitative assessment.

In this paper, the regional model setup is explained in Sect. 2; the verification data and verification method are presented in Sect. 3; and evaluation of downscaled results for seasonal mean as well as interannual variability is shown in Sect. 4. In Sect. 5, we will discuss physical processes responsible for affecting RCM performance using additional sensitivity experiments. Section 6 is the conclusion.

2 Model description

The regional atmospheric model adopted here is the WRF-ARW version 3.0.1 (Skamarock et al. 2008) developed at the National Center for Atmospheric Research (NCAR). Horizontal mesh size is 54 km (90 × 80 grids) and the vertical grid number is 28 layers. Figure 1 shows the covered area. The WRF's short wave radiation parameterization is based on Dudhia (1989), and the long wave radiation scheme is the Rapid Radiative Transfer Model (Mlawer et al. 1997). Other physical parameterizations include cumulus convection scheme (Kain 2004), cloud microphysics scheme (Hong et al. 2004), non-local parameterization of the planetary boundary layer (Hong et al. 2006), MM5 similarity theory for the surface layer, and Simplified Simple Biosphere (SSiB) Model land surface (Xue et al. 1991, 2001). The SSiB is a biophysics-based model of land–atmosphere interactions and is designed for global and regional studies. It consists of three soil layers and one vegetation layer. The aerodynamic resistance values in SSiB are determined in terms of vegetation properties, ground conditions, and bulk Richardson number according to the modified Monin–Obukhov similarity theory. The model is intended to realistically simulate the controlling biophysical processes and to provide fluxes of radiation, momentum, and sensible and latent heat to RCMs.

The WRF is driven using atmospheric and surface forcing data obtained from NCEP-DOE reanalysis 2 (NCEP2; Kanamitsu et al. 2002). NCEP2 reanalysis 2 may not be the best reanalysis products for the East Asian climate (see discussions in next section). However, this study emphasizes how much value is added by the dynamical downscaling. We need to select the best reanalysis data as a reference to assess the model results. It is not necessary to select the best reanalysis data as a LBC. Four outmost rows of the grid points from the lateral boundary are nudged to the forcing dataset. The period of simulation is 11-year from 1993 through 2003. The initial time for each year's numerical integration is 25 May and the ending time is 1

September of the same year, covering the EASM period. The first 7 days are for spin-up and the latter 3 months (June, July, and August) are applied for analysis. Hereafter, the ensemble of the numerical experiments with the aforementioned setting is referred to as the CNTL run. In Sect. 5.1 we discuss the investigation on the uncertainty raised from the land surface processes. The sensitivity experiments, named NOAH and GSWP, will be introduced (See Sect. 5.1 for detail).

3 Verification data

We evaluate the downscaled results based on statistical measure using atmospheric variables and surface precipitation. The Asian Precipitation—Highly Resolved Observational Data Integration Towards the Evaluation of Water Resources (APHRODITE; Yatagai et al. 2009) is adopted as the truth for precipitation. The APHRODITE is a daily precipitation dataset on a 0.25-degree grid based on rain gauge measurements but with consideration of orographic enhancement.

Since there are a limited number of observations for the atmosphere, we have to adopt reanalysis data for evaluation of the atmospheric circulation simulation. However, there are substantial differences among several available reanalysis datasets. We believe that the GAME reanalysis data (Yamazaki et al. 2003) would be most reliable for the East Asian region because, in the GAME reanalysis, additional upper-air sounding conducted during the GAME intensive observing period in 1998 was incorporated and a high-resolution GCM was used for data assimilation (Yamazaki et al. 2003). The GAME reanalysis, however, covers only the warm season in 1998 corresponding to the intensive observation period. Therefore, we first evaluated three global reanalysis data, ERA-Interim (hereafter, ERA; Dee et al. 2011), JRA25 (Onogi et al. 2007), and NCEP2, using the GAME reanalysis data as a reference during June–July–August of 1998. The results show that all these reanalyses are generally closer to GAME reanalysis in the East Asian region. Table 1 lists the comparisons of reanalysis datasets for June–July–August in 1998 by using basic statistics of four meteorological indices (upper troposphere zonal wind, middle troposphere pressure height, lower troposphere temperature, and lower troposphere meridional moisture transport) over East Asia (85–120°E, 25–52°N), in which the GAME reanalysis is used as the truth. For every index, each reanalysis shows very high spatial correlation with the GAME reanalysis. Only for meridional moisture transport at 850 hPa, the NCEP2 shows slightly lower correlation. Meanwhile, JRA25 and NCEP2 have relatively large biases in the geopotential height at 500 hPa. The ERA data appear to be closer to the GAME reanalysis. Hereafter, this study uses ERA as the verification data of the atmospheric properties. We also check the root-mean-square-error (RMSE) and find the results are very consistent with the bias. Since the bias also shows positive and negative features, to make the discussion more concise, we only present the bias in this paper.

Table 1 Spatial pattern correlation (SC) and mean bias (BIAS) of circulation indices in ERA-Interim, JRA25, and NCEP2 against the GAME reanalysis over East Asia (85–120°E, 25–52°N) for JJA 1998

	SC	BIAS
ERA		
U200	1	0.37
H500	1	0.01
T850	1	0.14
vq850	0.97	−3.0
JRA		
U200	1	0.47
H500	1	1.27
T850	0.98	−0.06
vq850	0.98	−5.0
NCEP2		
U200	1	−0.28
H500	1	4.24
T850	0.98	0.27
vq850	0.94	−1.0

Indices are zonal wind speed at 200 hPa (U200, m s^{-1}), geopotential height at 500 hPa (H500, m), temperature at 850 hPa (T850, K), and meridional moisture flux at 850 hPa (vq850, g m kg^{-1} s^{-1})

4 Assessing dynamical downscaling

The JJA-mean atmospheric 200-hPa zonal wind and 500-hPa geopotential height of the ERA reanalysis averaged from 1993 through 2003 are shown in Fig. 2. The strongest upper level zonal wind is around 40°N, which corresponds to the westerly jet running to the north of the Tibetan Plateau. The core of the westerly jet is found around 80°–90°E (Fig. 2a). The tropical easterly jet in low troposphere is observed equator-ward at around 25°N (not shown). The contrast in zonal wind in the upper troposphere is associated with the Tibetan High centered around 30°N, which is maintained by diabatic heating resulting from deep convection in Southeast Asia as well as surface heating over the Tibetan Plateau (Hoskins and Rodwell 1995). In the middle troposphere at 500-hPa, zonal structure is evident to the north of 40°N, weakly meandering and having a ridge near 100°E and a trough near 120°E (Fig. 2b). The meandering feature of 500-hPa geopotential height is associated with a distribution of arid climate in mid-latitude Asia through a modulation of mid-latitude

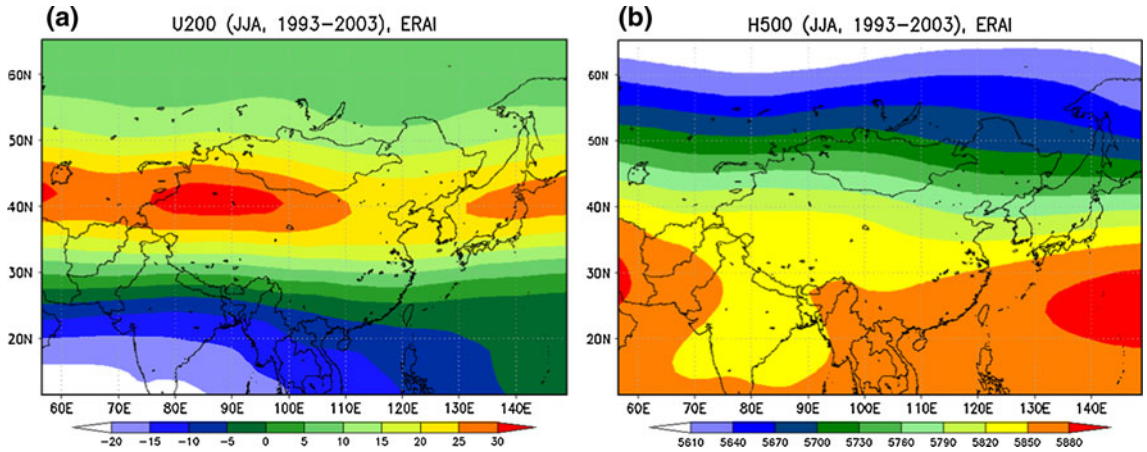

Fig. 2 Eleven-year (1993–2003) JJA mean **a** U200 (m s^{-1}) and **b** H500 (m) in ERA-Interim

storm activity due to large-scale orographic effects (Broccoli and Manabe 1992). The meridional gradient of geopotential height becomes weaker at lower latitudes. In the lower troposphere, temperature at 850 hPa shows a warmer area over the Middle East, North India, Central Asia, and Northern China, corresponding to the arid and semi-arid areas (not shown). Moisture transport in the lower troposphere, which is the most important feature in the convective process within the EASM, shows distinct northward moisture flow from the North Bay of Bengal and coastal regions over Southeast China as a result of conjunction of southwesterly flow from the Indian Monsoon and clockwise circulation due to the Western North Pacific subtropical High (Fig. 3).

4.1 Validation of dynamical downscaling of circulation

Figure 3 shows comparisons of upper-level zonal wind (U200), middle-level geopotential height (H500), and meridional moisture flux (vq850) for ERA, which is taken as a reference in this study, NCEP2 (LBC data), and CNTL (downscaled). The CNTL results in Fig. 4 are from the average of the 11-year simulations. Long-term mean structures for U200 in ERA and NCEP2 are very similar as spatial correlation reaches 0.99 (Table 2). In CNTL, however, the westerly jet core along with the associated minimum wind center appears further to the west. Meanwhile, the high wind speed center over the Philippian area as shown in the reanalyses is extended northwest onto the continent in CNTL. These deficiencies lead to lower spatial correlation and large biases for the 200-hPa zonal wind. In contrast, CNTL captures the spatial pattern in middle tropospheric geopotential height as the correlation coefficient is 0.96. Meanwhile, it also produces a lot of small-scale spatial variability corresponding to its relatively high resolution compared with reanalyses (Fig. 3). The simulated northern part of the southwest-northeast oriented trough axis, however, shifts much to the west, resulting in low geopotential height appearing in northern China and Mongolia and contributing to the significant negative bias (Table 2). The CNTL run has a large cold bias in temperature at 850 hPa. The comparison indicates that dynamical downscaling in this study over East Asia does not successfully add value to the forcing reanalysis data in terms of the atmospheric structure in the upper and middle troposphere, which is consistent with previous studies using simulations of a few years (e.g., Castro et al. 2005; Gao et al. 2011).

On the other hand, the downscaled meridional moisture transport at 850 hPa (vq850), which is crucially important for EASM precipitation activity, retains a similar spatial correlation to the driving reanalysis, in which 11-year mean correlation coefficients are 0.82 and 0.81 for NCEP2 and CNTL, respectively (Table 2). Mean bias in vq850, however, is significantly reduced according to the downscaling (Table 2). The value added in low-level meridional moisture transport has also been found in other downscaling studies (e.g., Xue et al. 2007). It should be pointed out that to assess the model's ability to improve interannual variability, the 11-year statistics are based on every year's statistics and then the averages of these results are reported in Table 2 (and other similar tables in this paper). Table 2 demonstrates that dynamical downscaling is likely to improve the simulation of the vq850 pattern's interannual variability. Considering the fact that the vq850 is a crucial factor affecting the convective activity in EASM, it is expected that the JJA precipitation in East Asia may have robust improvement due to dynamical downscaling.

4.2 Verification of dynamical downscaling of precipitation

Many studies have suggested that dynamical downscaling improves the spatial pattern of warm season rainfall due to

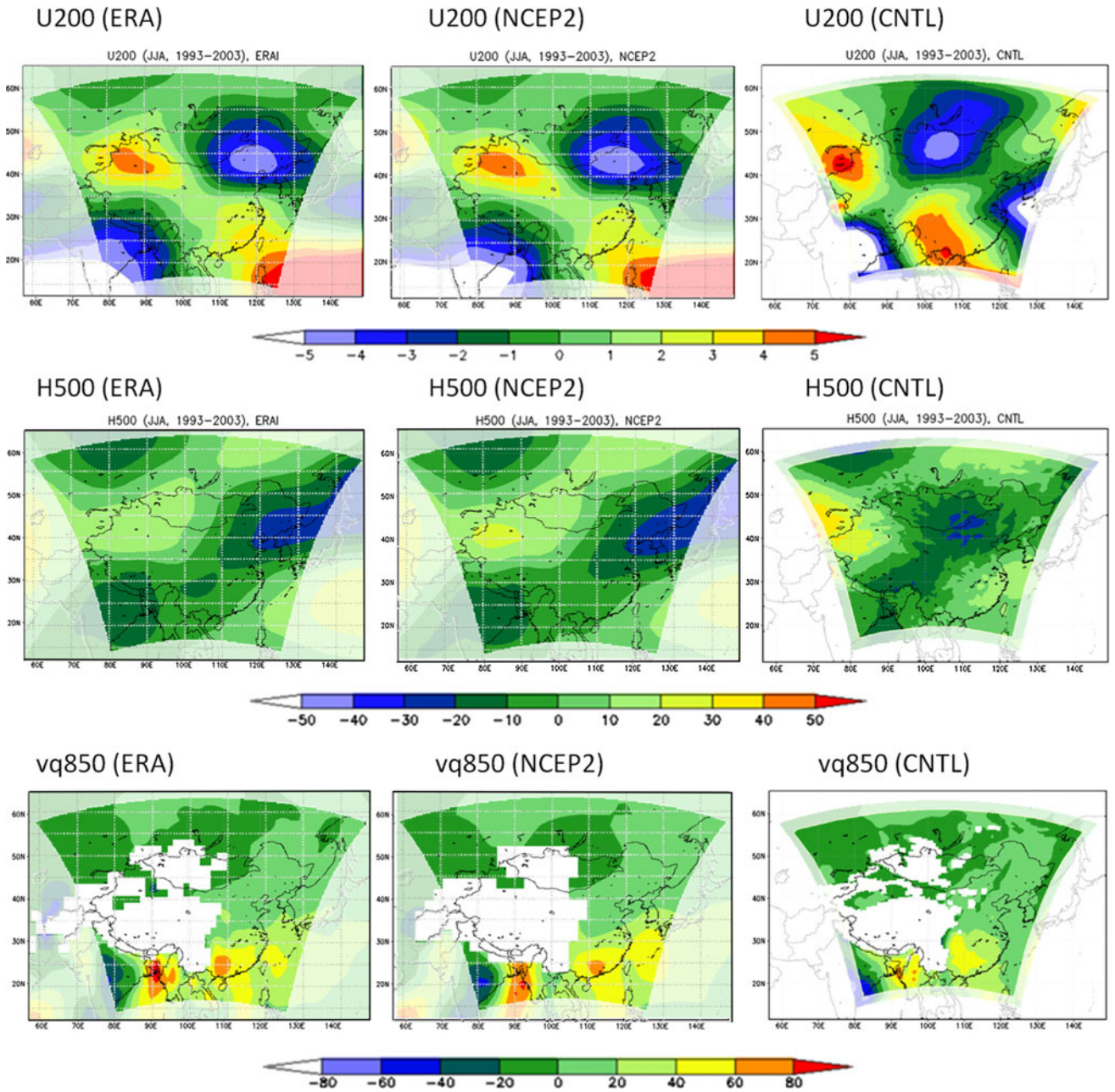

Fig. 3 Eleven-year (1993–2003) JJA mean U200 (*top*, m s^{-1}), H500 (*middle*, m), and vq850 (*bottom*, g m kg^{-1} s^{-1}) in ERA-Interim (*left*), NCEP2 (*middle*), and CNTL run (*right*). Zonal mean of U200 and H500 are removed in each figure

its high resolution for topography and/or physical representations (e.g., Christensen et al. 1998; Mo et al. 2000; Wang et al. 2003; Zhang et al. 2003; De Sales and Xue 2006; Sato et al. 2008). However, few studies (e.g., De Sales and Xue 2011) focused on the interannual variation of precipitation. In this section, we will analyze downscaled precipitation for each year in order to clarify whether the RCM is capable of simulating interannual variation of EASM precipitation features that is controlled by interannual variation of large-scale circulations.

Figure 4 illustrates 11-year JJA-mean precipitation in the observation (APHRODITE), NCEP2, and CNTL. Obviously, precipitation in CNTL successfully captures detailed distribution of precipitation in East Asia that was originally absent in the reanalysis data, which agrees with previous studies (e.g., Xie et al. 2006; Sato et al. 2007b; De Sales and Xue 2011). NCEP2 significantly overestimates precipitation over southeastern Asia. The precipitation to the south of the Yangtze River in China also has a substantially wet bias, which was overcome in the CNTL.

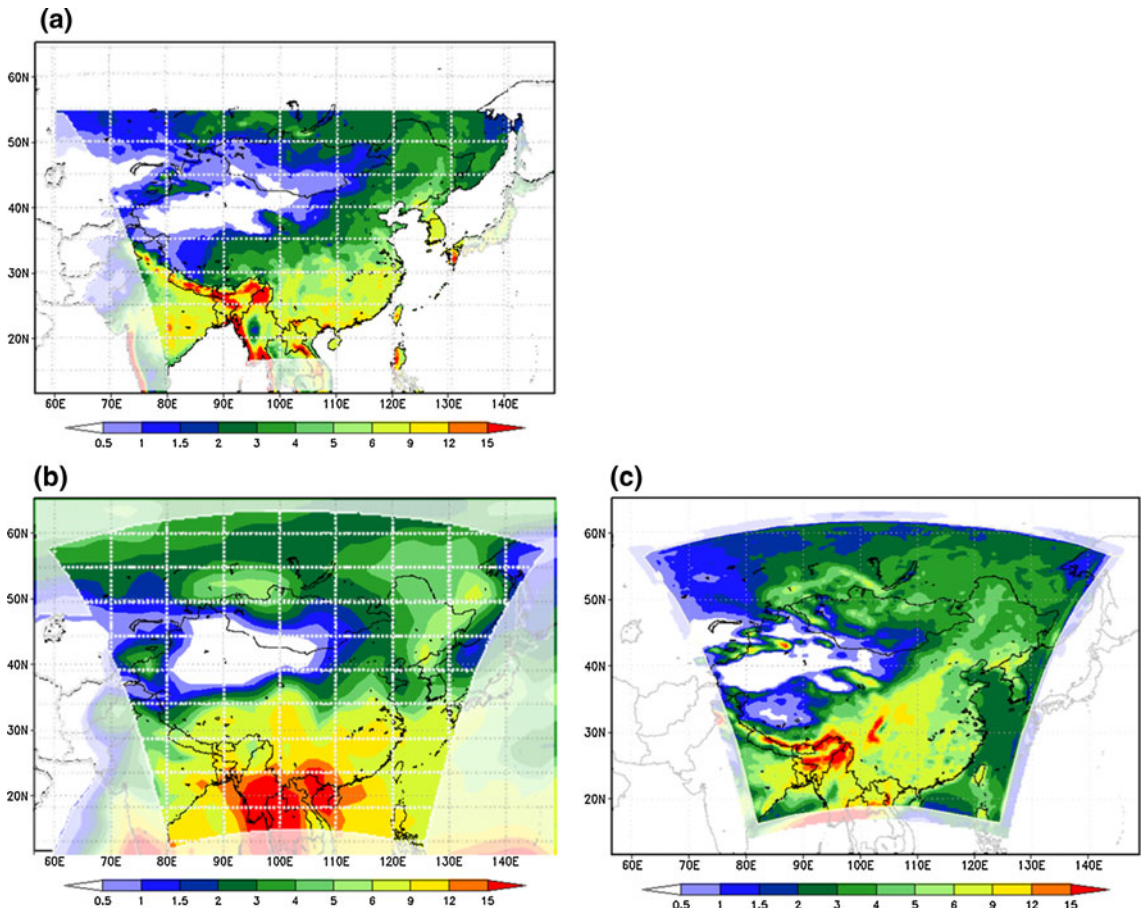

Fig. 4 JJA mean precipitation (mm day^{-1}) in **a** observation (APHRODITE), **b** NCEP2, and **c** CNTL run from 1993 to 2003

Table 2 Spatial pattern correlation (SC) and mean bias (BIAS) of circulation indices in NCEP2 and CNTL run against the ERA-Interim over East Asia (85–120°E, 25–52°N) during JJA over 1993–2003

	SC	BIAS
NCEP2		
U200	0.99	−0.48
H500	0.99	4.89
T850	0.97	0.22
vq850	0.82	6.69
CNTL		
U200	0.78	0.05
H500	0.96	−10.30
T850	0.71	−1.83
vq850	0.81	−1.04

SC and BIAS are expressed as the 11-year averages of SC and BIAS computed for each year, respectively. The units are the same as in Table 1

In particular, orographic enhancement of precipitation is found to be improved over the Himalayas and complex terrain over the Tibetan Plateau, as well as the Tian Shan Mountains located in Northwestern China. The meridional contrasting feature of aridity along North China and Mongolia is more accurately simulated in CNTL. NCEP2 overestimates the extremely arid area there. However, CNTL also shows some deficiencies in downscaling. Mean precipitation due to northeastward migration of EASM, for instance, is overestimated in CNTL, which causes stronger precipitation in the Huai River basin (between 30°N and 40°N). CNTL fails to reproduce high precipitation along the western coastal area in the eastern Bay of Bengal probably due to its location too close to the boundary. A spectacular amount of convective precipitation is simulated in the Bay of Bengal and northern Indochina Peninsula in CNTL, which is also the southern boundary of the domain. This feature is probably related to the WRF–ARW's LBC treatment in the tropical region. Furthermore, precipitation over the East China Sea is low compared to the Climate Prediction Center Merged Analysis of Precipitation (Xie and Arkin 1997 not shown).

The comparison of average JJA precipitation statistics in NCEP2 and CNTL is summarized in Table 3. The correlation coefficients are calculated against observation for each year from 1993 through 2003, and then mean correlation coefficient is calculated. Therefore, these statistics

also include the information of the interannual variability, which will be the focus of the next section. We have conducted the T test to check whether the differences between NCEP2 and CNTL are statistically significant. It turns out that except for the correlation difference in Northwest China and Southeast China, correlation differences in other subregions and bias difference in every subregion are statistically significant at more than a 90 % level. Among them the majority have more than 95 % significance level. Table 3 shows that the WRF produces higher spatial correlation with observation than NCEP2 for the whole domain, consistent with our discussion based on Fig. 4. However, the model has different downscaling ability over different subregions. Precipitation in North China deteriorates in the CNTL run with both lower spatial correlation and larger bias compared to the NCEP2. The bias in North China indicates that the rainfall along the Meiyu rainfall band was too strong, which might be responsible for the meridional position of the westerly jet axis and will be addressed in Sect. 5.2. Over the Mongolian domain the spatial pattern of precipitation is ameliorated, although the bias gets significantly larger, which also will be discussed later. Opposite to the Mongolian domain, the downscaled JJA precipitation in S.E. China produces lower bias but similar spatial correlation (very low) to the NCEP2. In N.W. China, which covers the northern part of the Tibetan Plateau and Loess Plateau, the spatial pattern of precipitation is slightly better in CNTL than NCEP2. Over the Tibetan Plateau, downscaled precipitation produces a significantly higher spatial pattern correlation with lower bias. By and large, the reduction of the wet bias or the increase in correlation in CNTL is robust even when we take the interannual variation into account.

Table 3 Spatial pattern correlation (SC) and mean bias (BIAS, mm day^{-1}) of JJA precipitation for 5 sub-domains in NCEP2 and CNTL run against the APHRODITE observation

	SC	BIAS
NCEP2		
Whole	0.61	1.00
Mongolia	0.63	0.50
S.E. China	0.29	3.04
N. China	0.64	0.69
N.W. China	0.80	0.36
Tibetan Plateau	0.06	3.88
CNTL		
Whole	0.65	1.23
Mongolia	0.69	1.36
S.E. China	0.29	−1.12
N. China	0.03	2.36
N.W. China	0.83	0.79
Tibetan Plateau	0.35	3.28

SC and BIAS are expressed as the 11-year averages of SC and BIAS computed for each year, respectively

4.3 Regional and interannual dependence of precipitation downscaling ability

To more closely evaluate the WRF's ability to downscale precipitation interannual variability, we examine the model performance over five subdomains with more comprehensive analyses.

4.3.1 The Mongolian subdomain

This section examines the effect of dynamical downscaling for each year over the Mongolian region, which is defined in the introduction. The dynamical downscaling over East Asia has the best performance in this region. Figure 5 shows the Taylor diagram (Taylor 2001) for JJA precipitation over Mongolia. In many studies, the Taylor diagram is used to investigate the difference of the model results relative to the reference data by showing spatial correlation and standard deviation after subtracting the mean of the atmospheric variables. The systematic bias is taken out. The precipitation deviation from its mean is then normalized with standard deviation of observed JJA precipitation in each year to make the results from different years more compatible. Therefore, the radial axis in Fig. 5 represents

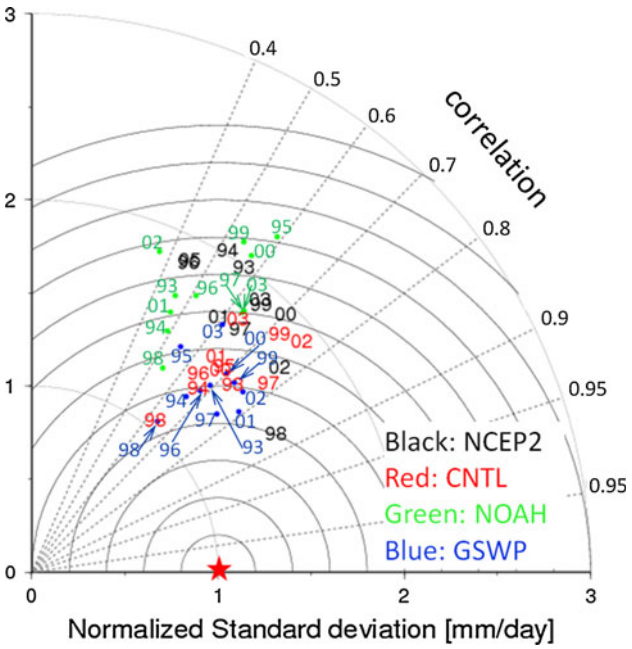

Fig. 5 Taylor diagram of JJA precipitation over Mongolia using observation (APHRODITE) as reference data (shown at *red star*). *2-Digit numbers* plotted in the diagram indicate the year analyzed. Normalized standard deviation is used to compare multiple years. *Black* for NCEP2, *red* for CNTL run, *green* for NOAH run, and *blue* for GSWP run, respectively

the normalized precipitation instead of the absolute precipitation amount in each year. The angle from the lateral axis indicates the pattern correlation, and the radius from the origin (0, 0) indicates the standard deviation against the observed precipitation's; i.e., the value 1 indicates that simulated and observed standard deviation are equal. The distance from the reference (APHRODITE's observation, red star) corresponds to the relative root mean squared error (RMSE). The 2-digit numbers shown in Fig. 5 correspond to the year evaluated. The two sensitivity experiments (NOAH and GSWP) are also plotted and will be discussed in Sect. 5. Two-digit numbers with different colors plotted in the diagram indicate the year analyzed with different experiments, respectively. For example, the years with red colors (CNTL) are clearly separated from the years with black colors (NCEP2). In most years, the RMSE and pattern correlation in CNTL are better than in NCEP2. Further analysis indicates that the downscaling performance is associated with ability to simulate interannual variation of the JJA mean precipitation over Central Mongolia. With careful comparison for each year, the effect of dynamical downscaling is classified into two groups—the years with significant improvements (1993, 1994, 1995, 1996, 1997, and 2000) and the years with no improvements (1998, 1999, 2001, and 2002)—which indicates that the effect of dynamical downscaling for the Mongolian region precipitation depends on the targeting year, and hence, to make an objective evaluation, the verification of downscaling ability should be conducted for multiple years.

To identify under what conditions the RCM causes better downscaling, we delineate the interannual variation of JJA precipitation over Mongolia (Fig. 6). The summers of 1999, 2001, and 2002 have the lowest precipitation during the period of this study. It seems the dynamical downscaling over Mongolia does not induce meaningful improvement for those dry summers. It has been suggested that the lower performance for those dry years is attributed to the treatment of land surface processes since the effects of soil moisture and evapotranspiration become more important under dry conditions than those expected under wet conditions (Koster et al. 2004; Guo et al. 2006; Fischer et al. 2007). In Sect. 5.2, further discussion is conducted with two sensitivity experiments on this issue.

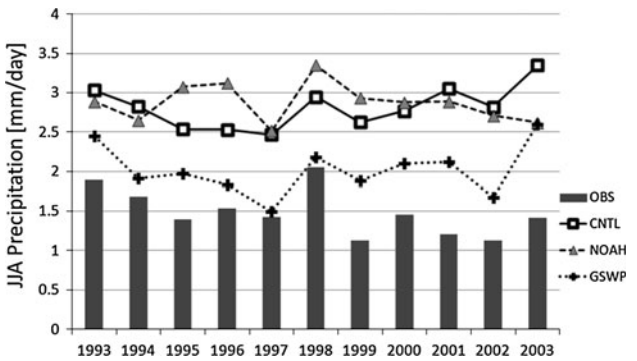

Fig. 6 Interannual variation of JJA precipitation (mm day^{-1}) in Mongolia for observation (APHRODITE) and three experiments

On the other hand, the simulated precipitation pattern deteriorates in 1998 despite abundant precipitation in Mongolia during the summer. It is well known that the EASM in 1998 brought massive precipitation in many areas in East Asia (Wang et al. 2003). Precipitation in eastern Mongolia was also very large during the JJA summer (not shown). However, the WRF fails to simulate northward migration of the Meiyu/Baiu front in 1998, which affects precipitation scores in the Mongolian region in 1998 in CNTL. Despite the deficiency in simulating the precipitation amount, however, the simulated standard deviation is improved and the RMSE remains about the same (Fig. 5).

In summary, the RCM is capable of improving JJA precipitation in Mongolia in normal and most wet years. In contrast, the dynamical downscaling ability is limited in dry years, which may be attributed to surface processes in the RCM and will be discussed later.

4.3.2 Four other subdomains

In the other four subregions, the improvement and the relationship between WRF downscaling ability and dry/wet years are not as clear as in the Mongolian subregion. Figure 7 shows the Taylor diagram of JJA precipitation for the other four subdomains and shows that the WRF generally has better simulations than NCEP2 Reanalysis in S.E. China, N.W. China, and the Tibetan regions. Over S.E. China, dynamical downscaling has the best performance among these four regions. It improves standard deviation for all 11 years and pattern correlation for six out of 11 years. Only 1 year's correlation gets worse. In N. China, the WRF has the worst performance. Both RMSE and spatial correlation get worse after dynamical downscaling (Fig. 7b). Over S.E. China and N. China, southerly wind is dominant during the EASM. Since S.E. China is located upstream of the southerly wind and closer to the southern lateral boundary, the imposed LBC may help the precipitation downscaling. Different from the Mongolian region, the precipitation in N. China very much depends on the EASM's northward movement. Its adequate simulation is very challenging and the WRF apparently fails to produce this feature well. The deficiency in simulation of the upper level jet may also affect the precipitation simulation in N. China.

In the two western regions, the downscaling makes improvements in some aspects but no improvement or even

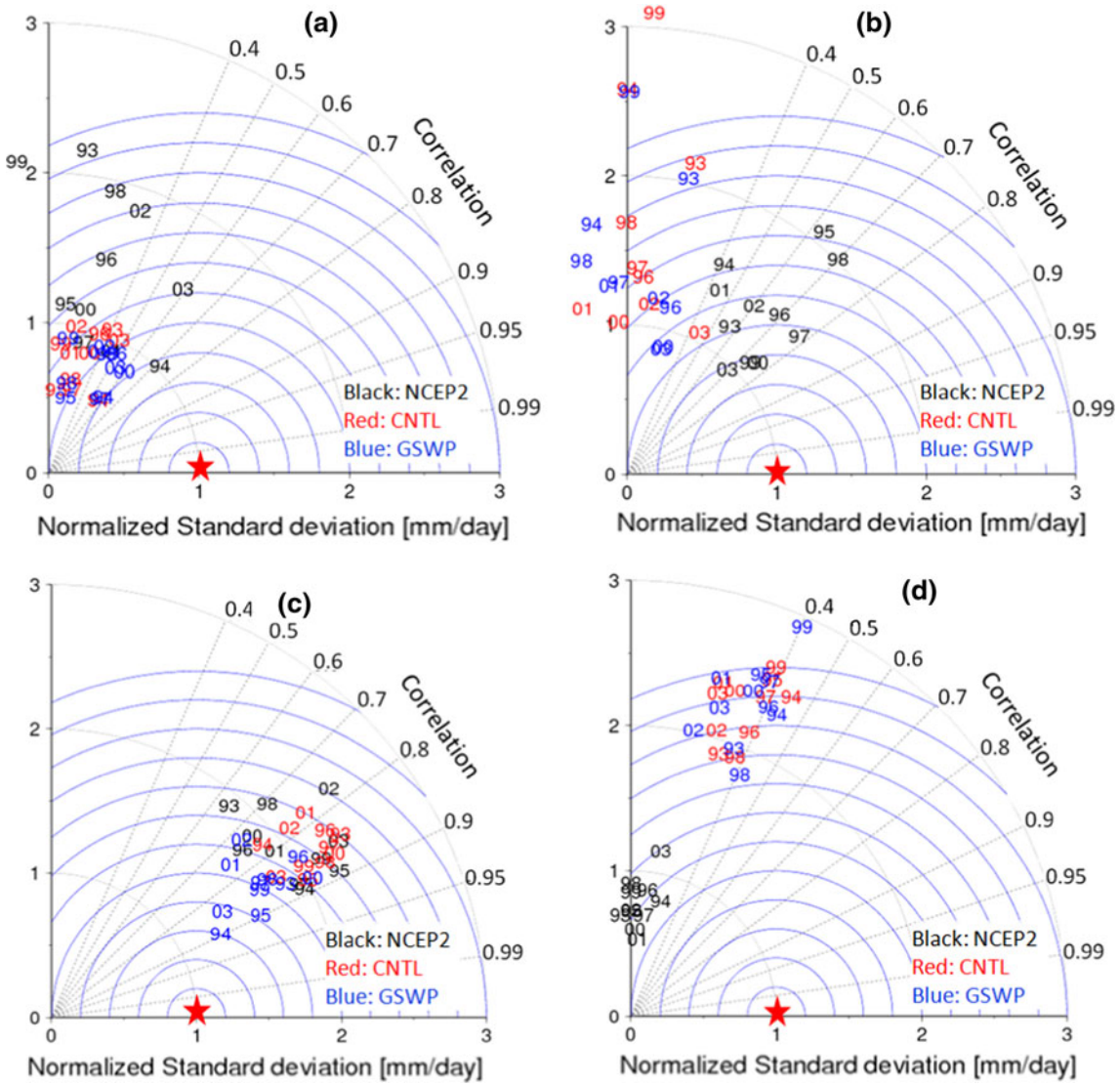

Fig. 7 As in Fig. 5, but for **a** S.E. China, **b** N.E. China, **c** N.W. China, and **d** Tibetan Plateau. *Black* for NCEP2, *red* for CNTL run, and *blue* for GSWP run

deterioration in other aspects. The spatial correlation of JJA precipitation in N.W. China (Fig. 7c) is slightly improved in five out of 11 years. Meanwhile, the standard deviation and RMSE are similar. Downscaled precipitation has improved spatial correlation in the Tibetan Plateau for all 11 years, but standard deviation is too high and RMSE is also larger in CNTL than NCEP2 (Fig. 7d). Better representation of complex terrains in the RCM should help better CNTL's simulation of precipitation pattern in the Tibetan Plateau.

The precipitation bias for individual year is investigated. In N. China, N.W. China, and Tibetan Plateau, wet bias tends to be large in dry years, i.e., too much rainfall in dry years (not shown), which is similar to what we found in Mongolia (Fig. 6). Contrastingly, in S.E. China, dry bias is significant in wet years while the bias is relatively small in dry years (not shown). The precipitation bias depends on the year and the region. In addition, we also analyze the standard deviation for interannual variation of JJA precipitation for each sub-domain (Table 4). Consistent with the general improvements discussed above, the interannual variation of precipitation is much improved after dynamical downscaling except for S.E. China, which suggests that dynamical downscaling plays a role in improving the simulation of the summer precipitation interannual variation. This discovery is different from another downscaling study (De Sales and Xue 2012), in which the 22-year winter prediction for North America from the NCEP Climate Forecast System is downscaled. De Sales and Xue (2012) have found that although the RCM improves the spatial distribution and intensity of precipitation substantially, there is no improvement in interannual variability.

Table 4 Standard deviation for interannual variation of JJA precipitation (mm day^{-1}) over 5 sub-domains in observation (APHRODITE), NCEP2, and CNTL run, respectively

	Obs	NCEP2	CNTL
Mongolia	0.30	0.43	0.27
S.E. China	1.10	1.28	0.81
N. China	0.90	1.13	0.97
N.W. China	0.12	0.26	0.19
Tibetan P.	0.57	1.12	0.64

Whether this is due to different domains, seasons, or imposed LBCs requires further investigation with more models.

5 Discussion

5.1 Influence of land surface processes during dry years

Figure 5 shows that downscaled precipitation has no improvement in relatively drier years such as 1999, 2001, and 2002. In fact, low precipitation in summer of 2002 was the most serious of the last few decades, having caused severe drought in Mongolia (Natsagdorj and Dagvadorj 2010). Land surface processes have been considered as a major factor that affects RCM downscaling (Xue et al. 2001, 2004). Because East Asia has been identified as one of the regions having strongest land–atmosphere interactions (Xue et al. 2010b), we conduct an additional experiment to clarify the role of land surface processes in downscaling in East Asia. Two sensitivity experiments are conducted. Firstly, NCEP2-derived initial soil moisture is replaced by soil moisture based on the Second Global Soil Wetness Project (GSWP-2, Dirmeyer et al. 2006) in order to verify the sensitivity of downscaling ability to initial soil moisture data (referred to as GSWP experiment). Initial soil moisture has been considered to have a strong effect on precipitation downscaling (e.g., Pielke et al. 1999). Secondary, the SSiB land surface scheme is replaced with Noah-LSM (referred to as NOAH experiment. Chen and Dudhia 2001) to investigate the uncertainty of precipitation downscaling due to land surface schemes.

In the GSWP-2 13 land surface models participated in a 10-year simulation with observed climate and reanalysis forcing (Dirmeyer et al. 2006). Due to data availability, in this study we used multi-model ensemble monthly mean climatology (1986–1995) soil moisture in May as the initial condition for the GSWP run. The multi-model ensemble means normally show better climate representation unless systematic biases for every model exist (Xue et al. 2010a). Since it is difficult to accurately measure soil moisture at the continental scale from ground and satellite observations, we consider the climatology of the GSWP-2 as the best available data set. The comparison of soil moisture between GSWP-2 and NCEP2 (Fig. 8) shows that the soil moisture in NCEP2 reanalysis (hence CNTL initial condition) is apparently wetter than the GSWP-2's estimation. In particular, initial soil moisture in GSWP over N.W. China and Mongolia is drier than that in CNTL by more than 20 %. Over dry regions around N. China and Mongolia, column-integrated soil moisture in GSWP-2 is 0.2 kg m^{-2} less than in the NCEP2 (0.60 kg m^{-2} for N. China and 0.46 kg m^{-2} for Mongolia, respectively, in NCEP2). Since the soil moisture anomaly has substantial influence on precipitation in arid and semi-arid regions (Guo et al. 2006), it is necessary to test whether the initial soil moisture in CNTL is responsible for the large precipitation bias over Mongolia in CNTL (Table 3).

Figure 5 shows the Taylor diagram for three experiments: CNTL, GSWP, and NOAH over the Mongolian region. The results from the GSWP experiment apparently show the best performance. Over the Mongolian region, more than 80 % of precipitation during May to October in 1998 comes from the evaporation around that area (Yoshimura et al. 2004). Sato et al. (2007a) has also shown that a large portion of atmospheric moisture is supplied as a result of evapotranspiration from the land surface over inland areas like Mongolia. By analyzing moisture sources around Northeast Asia, Sato et al. (2007a) found that one-third of atmospheric moisture was maintained by local evapotranspiration in Mongolia. The largest contributor is evapotranspiration in upstream regions such as Siberia. Therefore, accurate evapotranspiration over inland areas is crucial for higher precipitation scores. In contrast, the contribution of local evapotranspiration becomes smaller in N. China and S.E. China as larger amounts of moisture are supplied from tropical oceans by EASM flow (Sato 2009), which should partially explain the WRF downscaling performance discussed in Sect. 4.

Figure 6 shows that wetter initial soil moisture in CNTL produces overestimated JJA precipitation while corrected (lower) initial soil moisture brings reasonable precipitation in the GSWP run and reduces the RMSE (Fig. 5). Meanwhile, spatial pattern correlation is also improved owing to the initial soil moisture correction. Figure 9 shows differences in surface fluxes between the GSWP and CNTL runs. In the GSWP run latent heat flux is significantly reduced because of less initial soil moisture; then more energy is partitioned into sensible heat flux in almost all areas in East Asia. The amount of latent heat decrease is most prominent in Mongolia, N. China, and N.W. China where soil moisture is very low (Fig. 8). This means that initial soil moisture reduction in the GSWP run strongly limits the moisture supply to the atmosphere in the semi-arid and arid

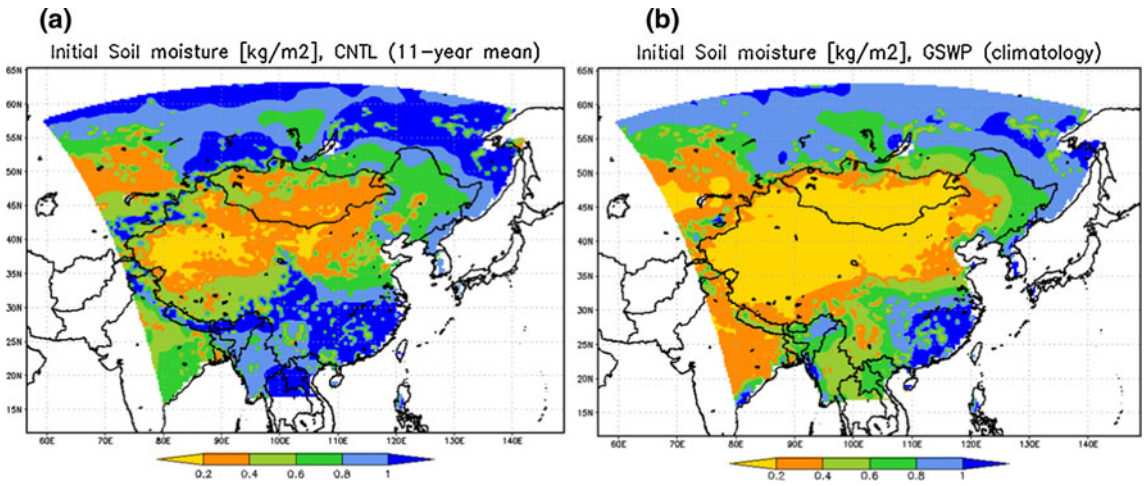

Fig. 8 Column total soil moisture (kg m^{-2}) at the initial state of experiment in **a** CNTL and **b** GSWP run. Since 6-hourly soil moisture data at 25 May every year is used in CNTL, **a** is shown as 11-year mean at 25 May

drylands. Figures 5 and 7 show that the initial soil moisture effect is more important in Mongolia and N.W. China than in other sub-domains. In these two regions, the results from the GSWP runs are clearly separated from other runs and NCEP2. These two regions are located in inland/high altitudes where moisture supply from the ocean is hard to reach. The contribution ratio of land evapotranspiration to total atmospheric moisture should be relatively large compared to other sub-domains. In other words, sensitivity of precipitation to initial soil moisture depends on the moisture recycling ratio. Additionally, a large moisture gradient between land and atmosphere (i.e., dry atmosphere and wetter soil) efficiently releases water from the vegetation surface toward the atmosphere. This supports the fact that the GSWP run has a significant improvement in performance in dry years (such as 1999, 2001, and 2002) while CNTL run fails to add value to the forcing reanalysis data.

To more clearly demonstrate the effect of initial soil moisture on dry years, the precipitation and moisture flux anomaly patterns in JJA 2002 are shown in Fig. 10. The precipitation in 2002 was very low compared to the 11-year climatology. It was less than 50 % compared to climatology in Central Mongolia. In the CNTL run, the observed anomalous pattern is not properly simulated (Fig. 10b). With the initial soil moisture correction, the GSWP run captures the anomalous precipitation pattern around Central Mongolia in 2002 (Fig. 10c). The initial soil moisture has a strong impact on the local water recycling. But its effect on the synoptic-scale circulation pattern is unclear (not shown).

Although the absolute value of the Mongolian precipitation is closer to observation in the GSWP run than in CNTL (Fig. 6), the precipitation in GSWP still overestimates after 1999, a dry period. This is probably due to the use of the 10-year average (1986–1995) soil moisture in the GSWP run. In dry years, such as 1999, 2000, 2001, and 2002, soil moisture is expected to be lower than climatology. Therefore, it is desirable to use corrected soil moisture with interannual variation taken into account. In addition, interannual variation of land surface conditions, such as albedo, vegetation fraction, and roughness, would be important since some studies have pointed out the influences of land surface parameters on interannual variability of precipitation (Park and Hong 2004; Li and Xue 2005; Kang et al. 2007).

In the land scheme experiment, the runs for the NOAH experiment are clearly separated from the CNTL (Fig. 7) with less improvement from the reanalysis data, which suggests that land surface scheme has a deterministic effect on the performance of the precipitation downscaling, particularly in dry areas like Mongolia. However, the soil moisture effect in this area is larger than the land scheme effects (Fig. 6). Since the land model in NCEP2 is the predecessor of NOAH, the close performance between NCEP2 and NOAH again confirms the land processes' crucial role in regional climate downscaling. Over S.E. China and N. China, NOAH tends to have lower performance for spatial correlation (0.04 and −0.23, respectively) than CNTL but similar results for RMSE and standard deviation. Over N.W. China and the Tibetan Plateau, NOAH and CNTL show similar spatial correlation, but biases tend to be larger in NOAH (0.96 and 3.63, respectively). A comprehensive discussion for the causes of the differences between CNTL and NOAH is out of the scope and not the purpose of this paper. The results present here just indicate that the land surface process/parameterizations is one of the important causes that produced the diverse in the RCM performance. The experiments with different land schemes are preliminary. More experiments are required to comprehensively investigate the impact of land surface schemes on the ability of dynamical downscaling for long time scales.

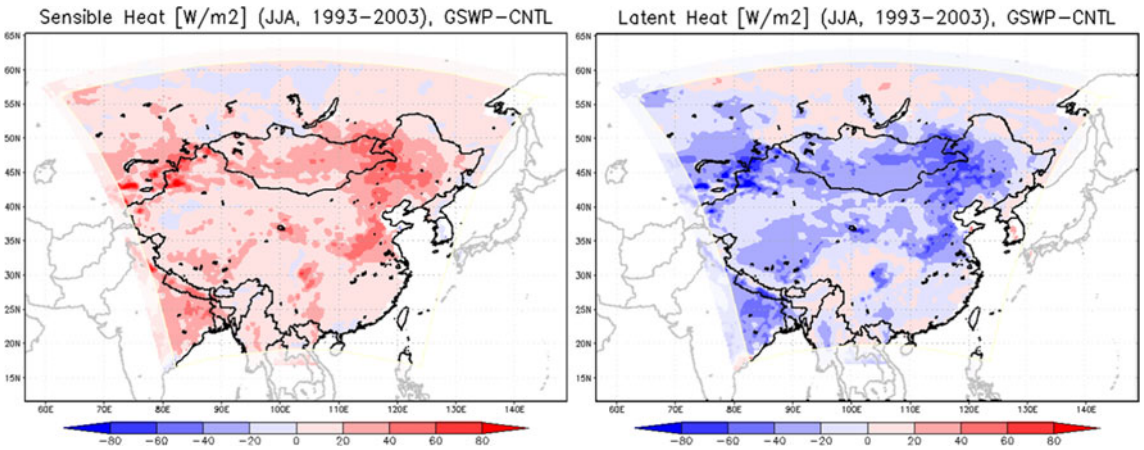

Fig. 9 11-year mean JJA sensible heat flux (W m^{-2}) and latent heat flux (W m^{-2}) differences between GSWP and CNTL experiments

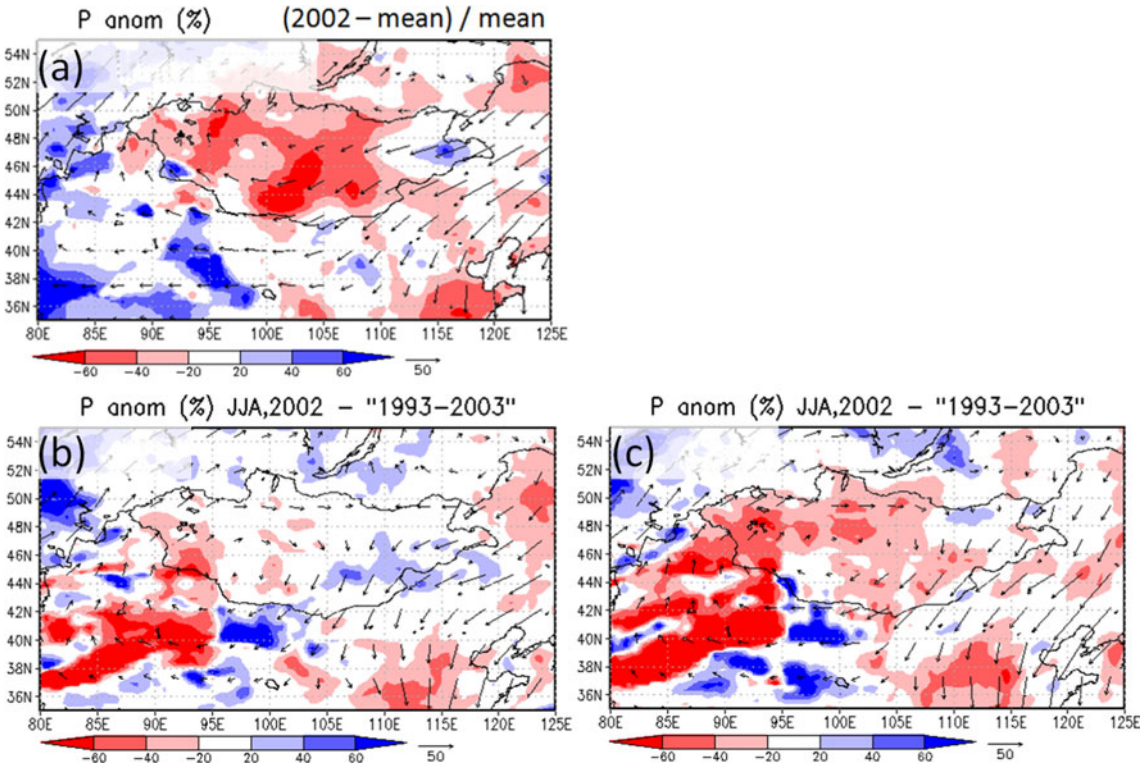

Fig. 10 Precipitation (mm $month^{-1}$) and vertical integrated moisture flux (kg m^{-1} s^{-1}) anomalies in JJA 2002 from 11-year JJA mean (1993–2003). Precipitation anomaly is expressed as ratio (%) against 11-year mean state. **a** Observation (APHRODITE), **b** CNTL run, **c** GSWP run. NCEP2 data are used to draw moisture flux in **a**

Re-initialization of atmospheric variables is a useful approach to improve precipitation scores around the N. China and N.W. China (e.g., Gao et al. 2011). The GSWP runs in this study suggest the re-initialization of soil moisture has the potential to improve the precipitation downscaling. Since the water recycling is an important process for precipitation in the arid region, the frequent correction of soil moisture has a role to ameliorate precipitation biases, especially for longer term simulations. The RCM requires sufficient spin-up duration in the arid regions when initial soil moisture contains biases because the adjustment of soil moisture takes a long time during dry condition. Our result suggests that the spin-up duration would be shortened in the arid regions if one can reduce biases in initial soil moisture. Further sensitivity studies are necessary to examine the relationship between the length of spin-up duration and precipitation downscaling.

5.2 Large-scale circulation and location of Baiu/Meiyu front

In Sect. 4.3.2, we confirmed that simulated precipitation along the Meiyu/Baiu front has very low spatial correlation (N. China, Fig. 7b), which is caused by an incorrect location of the precipitation belt along the Meiyu/Baiu front. This system is established under the complicated thermodynamic balance among southward cold air flow along the Baiu trough and lower-level humid southerly wind driven by the EASM and the Pacific high (e.g., Ninomiya and Akiyama 1992). Studies have found the role of the upper westerly jet to determine the location of the precipitation belt (e.g., Liang and Wang 1998; Yoshikane et al. 2001; Sampe and Xie 2010). We find that dynamical downscaling does not improve upper air large scale structures, such as zonal wind speed (Fig. 3; Table 2). Castro et al. (2005) also showed large errors in synoptic-scale circulation patterns in results from Type 2 downscaling. Thus, low performance for the Baiu/Meiyu rainfall band is probably attributed to the problem of adequate simulation of upper air circulation, especially in the westerly jet. Since the location of the westerly jet is determined by many different factors, such as interaction of zonal mean flow and mountain ranges, diabatic heating in the tropics and the Tibetan Plateau, and condensation heating along the Baiu/Meiyu front, it is difficult to simulate the position of the westerly jet axis even with sophisticated models. Some studies suggest a spectral nudging method (e.g., von Storch et al. 2000). Once position of the westerly jet is improved, location of the precipitation belt is expected to improve, which eventually leads to higher performance in the precipitation pattern in N. China. We conjecture that relatively lower performance in 1998 over Mongolia (Fig. 5) is also associated with the biases in large scale features. A great deal of effort must be carried out to study how to improve the mesoscale features by dynamical downscaling through the improvement of large-scale circulation patterns.

6 Conclusion

In this study, the application of dynamical downscaling for simulating East Asian summer regional climate and its interannual variability is examined using the WRF model. Simulations driven by the NCEP reanalysis II are conducted for 11 years in order to investigate the possible influence of interannual variation on downscaling ability. Statistical analysis based on the downscaled data reveal that dynamical downscaling does not add value to large-scale features in the upper and middle troposphere while meridional moisture transport in the lower troposphere is improved after dynamical downscaling.

For precipitation over East Asia, it is confirmed that dynamical downscaling successfully improves the precipitation pattern over Mongolia and the Tibetan Plateau where precipitation is largely affected by topographic forcing and land–atmosphere interaction. Furthermore, interannual variation is well produced by dynamical downscaling in all sub-domains except for S.E. China. Over Mongolia, the performance in precipitation downscaling is strongly dependent on the year: the RCM is skillful for normal and wet years, but not skillful for dry years, which suggests that land surface processes play a dominant role in controlling downscaling ability.

A sensitivity experiment using GSWP-2-based soil moisture shows that precipitation bias is significantly reduced by using corrected initial soil moisture in comparison to the control experiment which uses NCEP2-derived soil moisture as an initial condition. The experiment also suggests that the correction of initial soil moisture is necessary to improve precipitation scores for dry years, for which simulation originally failed. Another sensitivity experiment using different land surface schemes suggested that precipitation downscaling skill in inland areas is very sensitive to the parameterizations of the land surface processes.

Analysis for the sub-domains indicates that precipitation features in N. China are the most difficult to improve by dynamical downscaling because the location and activity of the Meiyu/Baiu front is closely associated with both lower-level meridional moisture transport and upper-level structures. It is necessary to have a realistic upper-air circulation pattern in the RCM as well as lower-level moisture transport in order to improve the self-organized convective rainfall band in East Asia over that region. Further studies are necessary to improve the RCM's performance for large scale circulation.

Acknowledgments The APHRODITE dataset was obtained at the project's web site (http://www.chikyu.ac.jp/precip/). This study was funded by the Environment Research and Technology Development Fund S-8-1(2) of the Ministry of the Environment, Japan, the Research Program on Climate Change Adaptation (RECCA) of the Ministry of Education, Culture, Sports, Science and Technology, Japan, and the National Science Foundation under grants AGS-1115506 and ATM-0751030. TS was supported by the excellent young researcher overseas visit program funded by JSPS for visiting to UCLA. The NCAR super computer has been used for the computation for this paper. We also appreciate the help of Dr. Fernando De Sales in this study.

References

Broccoli AJ, Manabe S (1992) The effects of orography on midlatitude northern hemisphere dry climates. J Clim 5:1181–1201

Castro CL, Pielke RA Sr, Leoncini G (2005) Dynamical downscaling: assessment of value retained and added using the Regional

Atmospheric Modeling System (RAMS). J Geophys Res 110:D05108. doi:10.1029/2004JD004721
Chen F, Dudhia J (2001) Coupling an advanced land surface/hydrology model with the Penn State/NCAR MM5 modeling system. Part I: model description and implementation. Mon Weather Rev 129:569–585
Christensen OB, Christensen JH, Machenhauer B, Botzet M (1998) Very high-resolution regional climate simulations over Scandinavia-Present climate. J Clim 11:3204–3229
De Sales F, Xue Y (2006) Investigation of seasonal prediction of the South American regional climate using the nested model system. J Geophys Res 111:D20107. doi:10.1029/2005JD006989
De Sales F, Xue Y (2011) Assessing the dynamic downscaling ability over South America using a precipitation verification approach. Int J Climatol 31:1205–1221. doi:10.1002/joc.2139
De Sales F, Xue Y (2012) Dynamic downscaling of CFS winter seasonal simulations over the United States using the ETA/SSIB-3 model. Clim Dyn. doi:10.1007/s00382-012-1567-x
Dee DP, Uppala SM, Simmons AJ, Berrisford P, Poli P, Kobayashi S, Andrae U, Balmaseda MA, Balsamo G, Bauer P, Bechtold P, Beljaars ACM, van de Berg L, Bidlot J, Bormann N, Delsol C, Dragani R, Fuentes M, Geer AJ, Haimberger L, Healy SB, Hersbach H, Hólm EV, Isaksen L, Kållberg P, Köhler M, Matricardi M, McNally AP, Monge-Sanz BM, Morcrette JJ, Park BK, Peubey C, de Rosnay P, Tavolato C, Thépaut JN, Vitart F (2011) The ERA-Interim reanalysis: configuration and performance of the data assimilation system. Q J R Meteorol Soc 137:553–597
Denis B, Laprise RL, Caya D (2003) Sensitivity of a regional climate model to the resolution of the lateral boundary conditions. Clim Dyn 20:107–126. doi:10.1007/s00382-002-0264-6
Dickinson RE, Errico RM, Giorgi F, Bates GT (1989) A regional climate model for western United States. Clim Change 15:383–422
Diffenbaugh NS, Ashfaq M, Shuman B, Williams JW, Bartlein PJ (2006) Summer aridity in the United States: response to mid-holocene changes in insolation and sea surface temperature. Geophys Res Lett 33:L22712. doi:10.1029/2006GL028012
Dirmeyer PA, Gao X, Zhao M, Guo Z, Oki T, Hanasaki N (2006) GSWP-2: multimodel analysis and implications for our perception of the land surface. Bull Am Meteorol Soc 87:1381–1397
Dudhia J (1989) Numerical study of convection observed during the winter monsoon experiment using a mesoscale two-dimensional model. J Atmos Sci 46:3077–3107
Fischer EM, Seneviratne SI, Vidale PL, Luthi D, Schar C (2007) Soil moisture-atmosphere interactions during the 2003 European summer heat wave. J Climate 20:5081–5099
Fu C, Wang S, Xiong Z, Gutowski WJ, Lee DK, McGregor JL, Sato Y, Kato H, Kim JW, Suh MS (2005) Regional climate model intercomparison project for Asia. Bull Am Meteorol Soc 86:257–266
Gao YH, Xue Y, Peng W, Kang HS, Waliser D (2011) Assessment of dynamic downscaling of the extreme rainfall over East Asia using a regional climate model. Adv Atmos Sci 28:1077–1098. doi:10.1007/s00376-010-0039-7
Giorgi F, Bates GT (1989) The climatological skill of a regional model over complex terrain. Mon Weather Rev 117:2325–2347
Giorgi F, Mearns LO (1999) Introduction to special section: regional climate modeling revisited. J Geophys Res 104:6335–6352
Giorgi F, Christensen J, Hulme M, Storch H, Whetton P, Jones R, Mearns L, Fu C, Arritt R, Bates B, Benestad R, Boer G, Buishand A, Castro M, Chen D, Cramer W, Crane R, Crossly J, Dehn M, Dethloff K, Dippner J, Emori S, Francisco R, Fyfe J, Gerstengarbe F, Gutowski W, Gyalistras D, Hanssen-Bauer I, Hantel M, Hassell D, Heimann D, Jack C, Jacobeit J, Kato H, Katz R, Kauker F, Knutson T, Lal M, Landsea C, Laprise R, Leung L, Lynch A, May W, McGregor J, Miller N, Murphy J, Ribalaygua J, Rinke A, Rummukainen M, Semazzi F, Walsh K, Werner P, Widmann M, Wilby R, Wild M, Xue Y (2001) Regional climate information—evaluation and projections, climate change 2001: the scientific basis. In: Houghton JT et al (eds) Contribution of working group to the third assessment report of the intergovernmental panel on climate change. Cambridge University Press, Cambridge, p 881
Gong W, Wang WC (2000) A regional model simulation of the 1991 severe precipitation event over the Yangtze–Huai River Valley. Part II: model bias. J Clim 13:93–108
Guo Z et al (2006) GLACE: the global land–atmosphere coupling experiment. Part II: analysis. J Hydrometeorol 7:611–625
Hong SY, Dudhia J, Chen SH (2004) A revised approach to ice microphysical processes for the bulk parameterization of clouds and precipitation. Mon Weather Rev 132:103–120
Hong SY, Noh Y, Dudhia J (2006) A new vertical diffusion package with an explicit treatment of entrainment processes. Mon Weather Rev 134:2318–2341
Hoskins BJ, Rodwell MJ (1995) A model of the Asian summer monsoon. Part I: the global scale. J Atmos Sci 52:1329–1340
Ishizaki NN, Takayabu I, Oh'izumi M, Sasaki H, Dairaku K, Iizuka S, Kimura F, Kusaka H, Adachi SA, Kurihara K, Tanaka K (2012) Improved performance of simulated Japanese climate with a multi-model ensemble. J Meteorol Soc Jpn 90:235–254
Kain JS (2004) The Kain-Fritsch convective parameterization: an update. J Appl Meteorol 43:170–181
Kanae S, Oki T, Musiake K (2001) Impact of deforestation on regional precipitation over the Indochina Peninsula. J Hydrometeorol 2:51–70
Kanamitsu M, Ebisuzaki W, Woollen J, Yang SK, Hnilo JJ, Fiorino M, Potter GL (2002) NCEP–DOE AMIP-II reanalysis (R-2). Bull Am Meteorol Soc 83:1631–1643
Kang HS, Hong SY (2008) Sensitivity of the simulated East Asian summer monsoon climatology to four convective parameterization schemes. J Geophys Res 113:D15119. doi:10.1029/2007JD009692
Kang HS, Xue Y, Collatz GJ (2007) Assessment of satellite-derived leaf area index datasets using a general circulation model: seasonal variability. J Clim 20:993–1015
Koster RD et al (2004) Regions of strong coupling between soil moisture and precipitation. Science 305:1138–1140. doi:10.1126/science.1100217
Li WP, Xue Y (2005) Numerical simulation of the impact of vegetation index on the interannual variation of summer precipitation in the Yellow River Basin. Adv Atmos Sci 22:865–876
Liang XZ, Wang WC (1998) Associations between China monsoon rainfall and tropospheric jets. Q J R Meteorol Soc 124:2597–2623
Liang XZ, Li L, Kunkel KE, Ting M, Wang JXL (2004) Regional climate model simulation of U.S. precipitation during 1982–2002. Part I: annual cycle. J Clim 17:3510–3529
Marbaix P, Gallee H, Brasseur O, van Ypersele JP (2003) Lateral boundary conditions in regional climate models: a detailed study of the relaxation procedure. Mon Weather Rev 131:461–479
Mlawer EJ, Taubman SJ, Brown PD, Iacono MJ, Clough SA (1997) Radiative transfer for inhomogeneous atmosphere: RRTM, a validated correlated-k model for the longwave. J Geophys Res 102(D14):16663–16682
Mo K, Kanamitsu M, Juang HMH, Hong SY (2000) Ensemble regional and global climate prediction for the 1997/1998 winter. J Geophys Res 105:29609–29623
Natsagdorj L, Dagvadorj D (2010) The adaptation to climate change in Mongolia. Ministry of Nature, Environment and Tourism of Mongolia, Ulaanbaatar, p 26 (in Mongolian)

Ninomiya K, Akiyama T (1992) Multi-scale features of Baiu, the summer monsoon over Japan and East Asia. J Meteorol Soc Jpn 70:467–495

Onogi K, Tsutsui J, Koide H, Sakamoto M, Kobayashi S, Hatsushika H, Matsumoto T, Yamazaki N, Kamahori H, Takahashi K, Kadokura S, Wada K, Kato K, Oyama R, Ose T, Mannoji N, Taira R (2007) The JRA-25 reanalysis. J Meteorol Soc Jpn 85:369–432

Park S, Hong SY (2004) The role of surface boundary forcing over south Asia in the Indian summer monsoon circulation: a regional climate model sensitivity study. Geophys Res Lett 31:12112. doi:10.1029/2004GL019729

Pielke RA Sr, Liston GE, Eastman JL, Lu L, Coughenour M (1999) Seasonal weather prediction as an initial value problem. J Geophys Res 104:19463–19479

Sampe T, Xie SP (2010) Large-scale dynamics of the Meiyu-Baiu rainband: environmental forcing by the westerly jet. J Clim 23:113–134

Sato T (2009) Influences of subtropical jet and Tibetan Plateau on precipitation pattern in Asia: insights from regional climate modeling. Quat Int 194:148–158. doi:10.1016/j.quaint.2008.07.008

Sato T, Kimura F (2007) Comparative study on the land-cover change and global warming impacts on regional climate in Northeast Asia. In: Proceedings of the 19th conference on climate variability and change, San Antonio, TX. Extended abstract available at http://ams.confex.com/ams/pdfpapers/117639.pdf

Sato T, Tsujimura M, Yamanaka T, Iwasaki H, Sugimoto A, Sugita M, Kimura F, Davaa G, Oyunbaatar D (2007a) Water sources in semi-arid Northeast Asia as revealed by field observations and isotope transport model. J Geophys Res Atmos 112:D17112. doi:10.1029/2006JD008321

Sato T, Kimura F, Kitoh A (2007b) Projection of global warming onto regional precipitation over Mongolia using a regional climate model. J Hydrol 333:144–154. doi:10.1016/j.jhydrol.2006.07.023

Sato T, Yoshikane T, Satoh M, Miura H, Fujinami H (2008) Resolution dependency of the diurnal cycle of convective clouds over the Tibetan Plateau in a mesoscale model. J Meteorol Soc Jpn 86A:17–31

Skamarock WC, Klemp JB, Dudhia J, Gill DO, Barker DM, Duda MG, Huang XY, Wang W, Powers JG (2008) A description of the advanced research WRF version 3. NCAR TECHNICAL NOTE, NCAR/TN–475+STR

Taylor KE (2001) Summarizing multiple aspects of model performance in a single diagram. J Geophys Res 106:7183–7192

Treadon RE, Petersen RA (1993) Domain size sensitivity experiments using the NMC Eta model. In: Proceedings of the 13th conference on weather analysis and forecasting, Vienna, VA, USA, pp 176–177 (preprints)

von Storch H, Langerberg H, Feser F (2000) A spectral nudging technique for dynamical downscaling purposes. Mon Weather Rev 128:3664–3673

Wang Y, Sen OL, Wang B (2003) A highly resolved regional climate model (IPRC-RegCM) and its simulation of the 1998 severe precipitation event over China. Part I: model description and verification of simulation. J Clim 16:1721–1738

Wang Y, Leung LR, McGregor JL, Lee DK, Wang WC, Ding Y, Kimura F (2004) Regional climate modeling: progress, challenges, and prospects. J Meteorol Soc Jpn 82:1599–1628

Warner TT, Peterson RA, Treadon RE (1997) A tutorial on lateral boundary conditions as a basic and potentially serious limitation to regional numerical weather prediction. Bull Am Meteorol Soc 78:2599–2617

Xie P, Arkin PA (1997) Global precipitation: a 17-year monthly analysis based on gauge observations, satellite estimates and numerical model outputs. Bull Am Meteorol Soc 78:2539–2558

Xie SP, Xu H, Saji NH, Wang Y, Liu WT (2006) Role of narrow mountains in large-scale organization of Asian monsoon convection. J Clim 19:3420–3429

Xu ZF, Yang ZL (2012) An improved dynamical downscaling method with GCM bias corrections and its validation with 30 years of climate simulations. J Clim 25:6271–6286. http://dx.doi.org/10.1175/JCLI-D-12-00005.1

Xue Y, Sellers PJ, Kinter JL, Shukla J (1991) A simplified biosphere model for global climate studies. J Clim 4:345–364

Xue Y, Zeng FJ, Mitchell KE, Janjic Z, Rogers E (2001) The impact of land surface processes on simulations of the U.S. hydrological cycle: a case study of the 1993 flood using the SSiB land surface model in the NCEP Eta regional model. Mon Weather Rev 129:2833–2860

Xue Y, Juang HMH, Li W, Prince S, DeFries R, Jiao Y, Vasic R (2004) Role of land surface processes in monsoon development: East Asia and West Africa. J Geophy Res 109:D03105. doi:10.1029/2003JD003556

Xue Y, Vasic R, Janjic Z, Mesinger F, Mitchell KE (2007) Assessment of dynamic downscaling of the continental U.S. regional climate using the Eta/SSiB regional climate model. J Clim 20:4172–4193

Xue Y, De Sales F, Lau KMW, Boone A, Feng J, Dirmeyer P, Guo Z, Kim KM, Kitoh A, Kumar V, Poccard-Leclercq I, Mahowald N, Moufouma-Okia W, Pegion P, Rowell D, Schubert SD, Sealy A, Thiaw WM, Vintzileos A, Williams S, Wu MLC (2010a) Intercomparison and analyses of the climatology of the West African Monsoon in the West African Monsoon Modeling and Evaluation Project (WAMME) first model intercomparison experiment. In special issue "West African monsoon and its modeling". Clim Dyn 35:3–27. doi:10.1007/s00382-010-0778-2

Xue Y, De Sales F, Vasic R, Mechooso CR, Prince SD, Arakawa A (2010b) Global and temporal characteristics of seasonal climate/vegetation biophysical process (VBP) interactions. J Clim 23:1411–1433

Xue Y, Vasic R, Janjic J, Liu YM, Chu PC (2012) The impact of spring subsurface soil temperature anomaly in the Western U. S. on North American summer precipitation—a case study using regional climate model downscaling. J Geophys Res 117:D11103. doi:10.1029/2012JD017692

Yamazaki N, Takahashi L, Yatagai A (2003) Report on the GAME reanalysis. GAME phase 1 summary reports. GAME publication 37, pp 81–87

Yatagai A, Arakawa O, Kamiguchi K, Kawamoto H, Nodzu MI, Hamada A (2009) A 44-year daily gridded precipitation dataset for Asia based on a dense network of rain gauges. SOLA 5:137–140

Yoshikane T, Kimura F, Emori S (2001) Numerical study on the Baiu front genesis by heating contrast between land and ocean. J Meteorol Soc Jpn 79:671–686

Yoshimura K, Oki T, Ohte N, Kanae S (2004) Colored moisture analysis estimates of variations in 1998 Asian Monsoon water sources. J Meteorol Soc Jpn 82:1315–1329

Zhang DL, Zheng WZ, Xue Y (2003) A numerical study of early summer regional climate and weather over LSA-East. Part I: model implementation and verification. Mon. Weather Rev 131:1895–1909